ELectronics EXpress

LETTER

IEICE Electronics Express, Vol.14, No.1, 1–12

A novel dual microwave Doppler radar based vehicle detection sensor for parking lot occupancy detection

Xinghe Bao[a)], **Yunlong Zhan**[b)], **Chang Xu, Kelu Hu, Chunlei Zheng, and Yingguan Wang**

Shanghai Institute of Microsystem and Information Technology, Chinese Academy of Science, No. 865, Changning Road, Shanghai, 200050, China

a) *baoxinghe123@163.com*

b) *qingqingzjin@126.com*

Abstract: This paper described a novel vehicle detection sensor design in which dual microwave Doppler radar transceiver modules were used to detect the movement of a parking vehicle. A motion recognition algorithm was also presented to identify the vehicle behavior and generate the parking space occupancy status. Comparing with existing methods such as magnetometer and optical based detection, the proposed design simplified engineering integration from complex optical system design as well as achieved a high detection accuracy. Experimental results showed that the proposed dual microwave Doppler radar sensor detected the vehicle movement clearly and the parking space occupancy detection accuracy was higher than 98%.

Keywords: microwave, Doppler radar, motion recognition, vehicle detection sensor, parking lot occupancy detection

Classification: Microwave and millimeter-wave devices, circuits, and modules

References

[1] J. Jermsurawong, *et al.*: "Car parking vacancy detection and its application in 24-hour statistical analysis," FIT (2012) 84 (DOI: 10.1109/FIT.2012.24).

[2] A. Kianpisheh, *et al.*: "Smart Parking System (SPS) architecture using ultrasonic detector," IJSEA **6** (2012) 51.

[3] C. Bai-gen, *et al.*: "The research and realization of vehicle detection system based on wireless magneto-resistive sensor," ICICTA (2009) 476 (DOI: 10.1109/ICICTA.2009.350).

[4] S. Lin, *et al.*: "A vision-based parking lot management system," IEEE SMC (2006) 2897 (DOI: 10.1109/ICSMC.2006.385314).

[5] S. S. Adhatarao, *et al.*: "Smart parking system for vehicles," IEEE VNC (2014) 189 (DOI: 10.1109/VNC.2014.7013341).

[6] H. Zhu, *et al.*: "A robust vehicle detection algorithm based on wireless sensor network," IEEE ICIST, (2014) 84 (DOI: 10.1109/ICIST.2014.6920337).

[7] B. Yang and Y. Lei: "Vehicle detection and classification for low-speed congested traffic with anisotropic magnetoresistive sensor," IEEE Sensors J. **15** (2015) 1132 (DOI: 10.1109/JSEN.2014.2359014).

DOI: 10.1587/elex.13.20161087
Received November 8, 2016
Accepted November 24, 2016
Publicized December 12, 2016
Copyedited January 10, 2017

[8] M. J. Caruso and L. S. Withanawasam: "Vehicle detection and compass applications using AMR magnetic sensors," Honeywell SSEC Tech. Papers, http://www.ssec.honeywell.com.
[9] Honeywell: "Application Note-AN218 Vehicle Detection Using AMR Sensors" (2005) http://www.honeywell.com.
[10] S. Lee, *et al.*: "Intelligent parking lot application using wireless sensor networks," IEEE CTS (2008) 48 (DOI: 10.1109/CTS.2008.4543911).
[11] X. Guan, *et al.*: "A vehicle detection algorithm based on wireless magnetic sensor networks," CHINACOM (2013) 669 (DOI: 10.1109/ChinaCom.2013.6694677).
[12] Z. Zhang, *et al.*: "A parking occupancy detection algorithm based on AMR sensor," IEEE Sensors J. **15** (2015) 1261 (DOI: 10.1109/JSEN.2014.2362122).
[13] S. Ma, *et al.*: "Reliable wireless vehicle detection using magnetic sensor and distance sensor," JDCTA **8** (2014) 112.
[14] J. Fang, *et al.*: "A low-cost vehicle detection and classification system based on unmodulated continuous-wave radar," IEEE ITSC (2007) 715 (DOI: 10.1109/ITSC.2007.4357739).
[15] J. L. Barker: "Radar, acoustic, and magnetic vehicle detectors," IEEE Trans. Vehic. Technol. **19** (1970) 30 (DOI: 10.1109/T-VT.1970.23429).
[16] J. E. Stevens and L. L. Nagy: "Diplex Doppler radar for automotive obstacle detection," IEEE Trans. Vehic. Technol. **23** (1974) 34 (DOI: 10.1109/T-VT.1974.23570).
[17] K. Tomiyasu: "Conceptual performance of bistatic Doppler radar for vehicle speed determination," IEEE Trans. Vehic. Technol. **30** (1981) 130 (DOI: 10.1109/T-VT.1981.23894).
[18] F. B. Berger: "The nature of Doppler velocity measurement," IRE Trans. Aeronaut. Navig. Electron. **ANE-4** (1957) 103 (DOI: 10.1109/TANE3.1957.4201534).
[19] Agilsense: "HB100 Datasheet," [Online] http://www.agilsense.com.
[20] Agilsense: "HB100 Application Note," [Online] http://www.agilsense.com.

1 Introduction

Recently, parking problems are becoming more and more serious in most cities. Therefore, intelligent parking lot management systems are being resorted to solve this problem [1]. A key point in these systems is the parking lot occupancy status acquisition, which is mainly achieved by employment of vehicle detection technologies such as ultrasonic, camera, magnetometer, and optical sensor [2, 3, 4, 5]. In these traditional detection methods, cable required systems, such as ultrasonic or camera based solution, has high detection accuracy but suffers from the inconvenience of installation and high infrastructure cost [6]. The magnetometer vehicle detect sensor, which is based on measurement of the earth's magnetic field disturbances caused by a vehicle, has advantages of easy installation, low cost and small size [7, 8, 9]. However, its detection accuracy could be easily influenced by environmental factors such as background magnetic field drifting, nearby ferromagnetic objects interference and difference of vehicle material [10, 11]. Therefore, many algorithms have been proposed for magnetometer vehicle detection. But reference [11] exposed that in the real situations, the vehicle detection success rates are usually less than 95%. Thus a Relative Extremum Algorithm

DOI: 10.1587/elex.13.20161087
Received November 8, 2016
Accepted November 24, 2016
Publicized December 12, 2016
Copyedited January 10, 2017

(REA) was proposed in this paper and the detection accuracy is above 98.8%. Although algorithms proposed in reference [11], as well as reference [6] and [12], achieved high detection rate, but they are based on a high sample rate of magnetometer, which will result in high battery power consumption. In order to improve the presence detection accuracy while keeping low power consumption, a second high accuracy detection method such as infrared or light sensor is expected to work with magnetometer operating at low duty cycle. However, the application of an optical sensor is limited by complicated component design, it could also be influenced easily by snow, leaves and dust [12, 13, 14].

This paper presented a dual microwave Doppler radar based vehicle detection sensor to detect the movement of a vehicle, and proposed a motion recognition algorithm to identify whether the parking space was occupied or not. The presented vehicle detection sensor was mounted in the center of a parking space. The movement of a vehicle coming or leaving the parking space would lead to Doppler frequency shift signal output from the two radar module in a specific timing sequence. Based on the output signals, the motion recognition algorithm would identify the behavior of the parking vehicle, and furthermore, generate the occupancy status of the parking space. Experiments of the vehicle movement detection and parking behavior identification were implemented in a parking lot through the proposed parking space occupancy sensor. As compared with traditional methods such as magnetometer and optical detection, the microwave detection is not easily affected by plastic shell, fallen leaves, snow, and dust as well as difference of vehicle material. The proposed design brought advantages in the elimination of detecting influence from environments, simplified system integration, and improved the detection accuracy significantly.

2 Microwave Doppler radar transceiver module

Microwave Doppler radar transceiver module is based on the principle of the Doppler Effect, which reveals that a moving target will lead to the reflected wave frequency change compared with the transmission signal. Principle of microwave Doppler radar movement detection was shown as Fig. 1. By transmitting a microwave beam toward a moving target and receiving the reflecting signal simultaneously, the high frequency transmission signal and a receiving signal were mixed to achieve an intermediate frequency (IF) signal, whose frequency is proportional to the velocity of the target [15, 16].

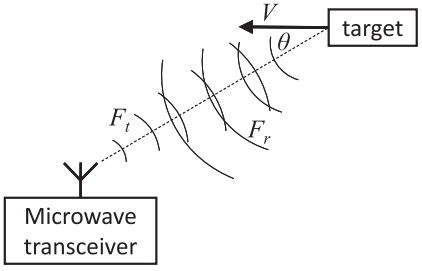

Fig. 1. Principle of microwave Doppler radar movement detection.

DOI: 10.1587/elex.13.20161087
Received November 8, 2016
Accepted November 24, 2016
Publicized December 12, 2016
Copyedited January 10, 2017

The difference of the wave frequency between the transmission and reflection is the Doppler frequency shift F_d.

$$F_d = |F_t - F_r| = 2 \times V \times \left(\frac{F_t}{c}\right) \times \cos\theta. \quad (1)$$

Where F_t is the transmit wave frequency, F_r is the reflect wave frequency, c is the speed of light (3×10^8 m/s), V is the velocity of detection target, and θ is the angle between the target moving direction and the wave beam transmission direction [17, 18]. In equation (1), if $V = 0$, then $F_d = 0$. This indicates that a microwave Doppler radar can detect a moving target but it will be blind to a static one.

The microwave Doppler radar transceiver module we used is HB100, from Agilsense company [19]. It is a 10.525 GHz X-Band Bi-static Doppler transceiver front-end module. The block diagram of HB100 is shown as Fig. 2. A Dielectric Resonator Oscillator (DRO), a microwave mixer and a pair of Micro-strip patch antenna array were built inside of the module. The "Tx" antenna were used to emit microwave beam, which will be reflected by the target in its transmission path. The reflected beam were received by "Rx" antenna. The transmission signal and reflection signal were mixed to output an intermediate frequency (IF) signal, whose value is related to the moving speed of the target.

Fig. 2. Block diagram of HB100 Doppler radar transceiver module.

The frequency setting of HB100 was 10.525 GHz with up to 20 dBm max radiated power supporting 10 to 15 meters detection range. A pair of 8 dBi micro-strip antenna were printed on HB100 to transmit and receive microwave signal. The radiation patterns of the antenna and their Half Power Beam Width (HPBW) were shown in Fig. 3. The azimuth 3 dB beam width was 80 degrees, and elevation 40

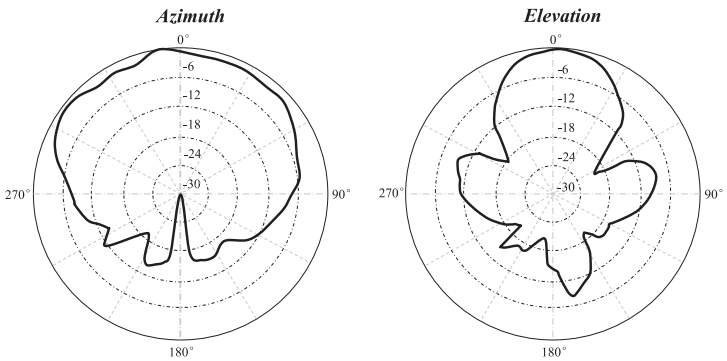

Fig. 3. Antenna beam pattern of HB100 Doppler radar module.

DOI: 10.1587/elex.13.20161087
Received November 8, 2016
Accepted November 24, 2016
Publicized December 12, 2016
Copyedited January 10, 2017

degrees. The power supply for HB100 was DC5V/30 mA. It was feasible to integrate it in a battery powered device where a second lower power sensor, for example a magnetometer, could be employed as a wake-up trigger to achieve lower power consumption but high detection accuracy [19, 20].

3 Design

3.1 Dual microwave Doppler radar sensor design

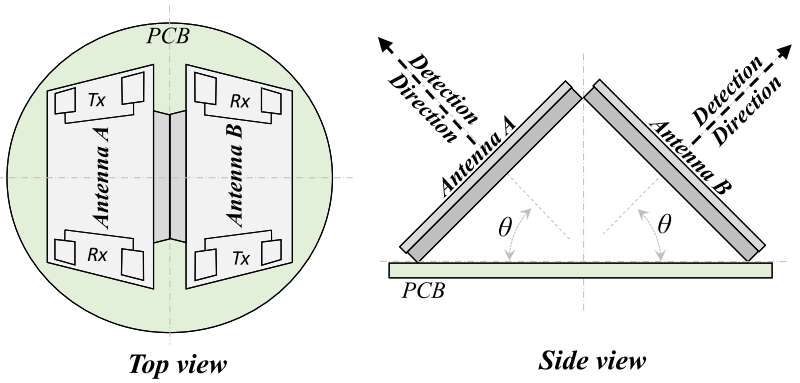

Fig. 4. Dual microwave Doppler radar sensor design.

According to the Doppler equation (1), a microwave Doppler radar is able to detect a moving target but it blind to a static one. The antenna beam pattern of HB100 module was shown as Fig. 3. The wave beam featured a good radiation direction. Based on these characteristics, as shown in Fig. 4, a vehicle detection structure was designed by employing two HB100 microwave Doppler radar transceiver modules assembled back-to-back. The two modules were combined and mounted on the PCB with their detection axis pointing to two opposite directions respectively. The angle between the detection direction and horizontal plan is θ. As shown in Fig. 5, since the sensor was designed to flush mounted in the ground, if θ is too small and near to 0, the microwave signal will be greatly attenuated by ground. On the other side, if θ is set close to 90 degree, according to equation (1), the Doppler frequency shift $F_d \approx 0$. The vehicle movement will be difficult to detect. In this design, the angle θ was set to 45 degree.

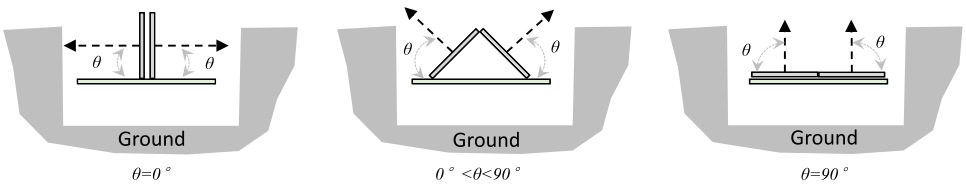

Fig. 5. Angle of setting two microwave Doppler radar sensor.

The radiation pattern of the dual microwave Doppler radar sensor was shown in Fig. 6. Since each radar module featured a directional microwave radiation, three detection sensitivity fields were formed upon the sensor as "F_A", "F_{AB}" and "F_B". A moving vehicle in the field of "F_A", or "F_B", would be detected by radar module "A", or "B", of the sensor, and by both "A" and "B" if it was in the field of "F_{AB}".

DOI: 10.1587/elex.13.20161087
Received November 8, 2016
Accepted November 24, 2016
Publicized December 12, 2016
Copyedited January 10, 2017

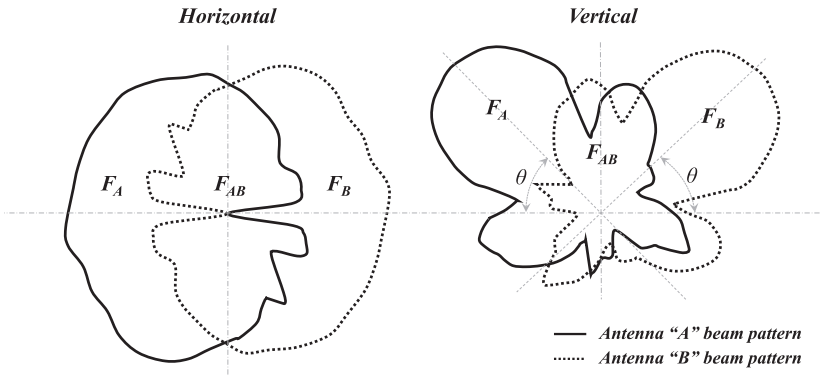

Fig. 6. Radiation pattern of the dual microwave Doppler radar sensor.

The movement of a vehicle coming or leaving the parking space would lead to Doppler frequency shift signal output from the two radar module following a specific timing sequence. The detection results would be input to a motion recognition algorithm to identify the behavior of the vehicle, and furthermore, generate the parking space occupancy status.

3.2 Circuit design

A symmetrical signal processing circuit structure was designed as in Fig. 7. Two identical microwave Doppler radar transceiver module HB100 were used. The output signal voltage magnitude of the two microwave Doppler radar module, V_{IFA}

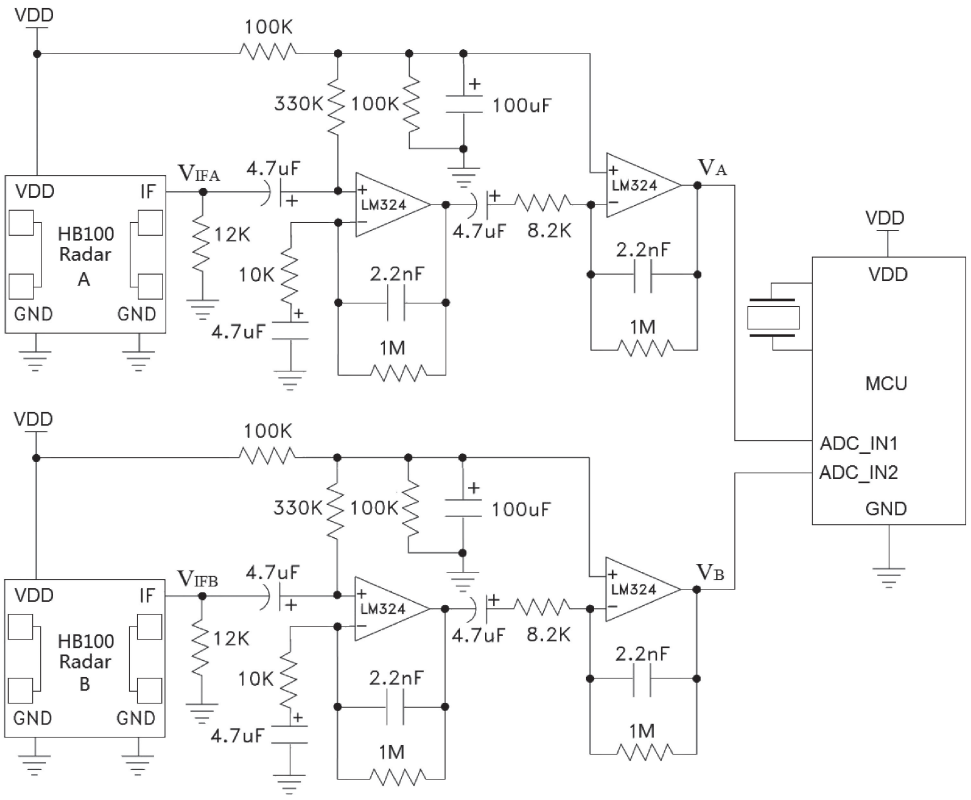

Fig. 7. Signal processing circuit of the dual microwave Doppler radar based vehicle detection sensor.

DOI: 10.1587/elex.13.20161087
Received November 8, 2016
Accepted November 24, 2016
Publicized December 12, 2016
Copyedited January 10, 2017

and V_{IFB}, was proportional to the reflection energy from detection target in range of 100 to 200 uV_{P-P}, depending on the target size and distance to HB100 [17]. Referring to the HB100 application guidance provided by Agilsense company [18], a two-stage high gain low frequency amplifier composed by two LM324s was employed for each module to amplify the Doppler frequency shift output signal, V_{IFA} and V_{IFB}, to a high voltage signal V_A and V_B, a processable level of 1 to 2 V, so that it could be sampled by the Analog-to-Digital Converter (ADC) of a MCU.

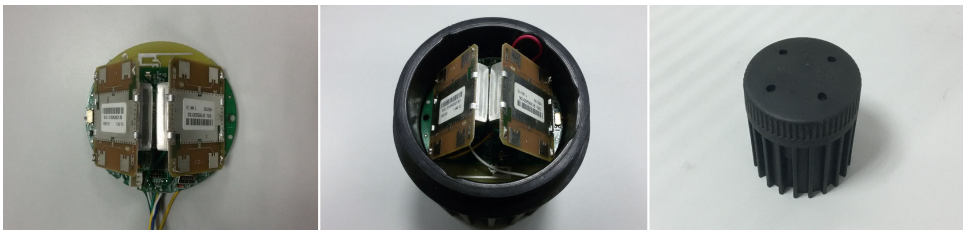

Fig. 8. Dual microwave Doppler radar based parking occupancy detection sensor.

Based on the dual microwave Doppler radar transceiver modules and its signal processing circuit design, a parking vehicle occupancy detection sensor was made to carry out our experiments. A plastic shell of Nylon with glass fiber, which is easy for the microwave transmission, was produced to assemble the PCB board and a battery pack. In order to meet the requirements of the parking occupancy sensor as a product, a magnetometer HMC5883L from Honeywell and a RF transceiver CC2530 form TI were also employed to achieve low power mode and Zigbee network connection. The product design of low power and Zigbee network will not be discussed in this paper.

3.3 Vehicle motion recognition algorithm

As described in the previous section, the two Doppler radar transceiver module radiated microwave beam to two opposite direction respectively. The detection space was divided into three independent fields, "F_A", "F_{AB}" and "F_B", as shown in Fig. 6. The field in which a vehicle was moving could be identified by the detection result of the related radar module. According to the detection results and process charging of all the three detection fields, the motion of a vehicle whether it was driving in or out of parking space could be identified.

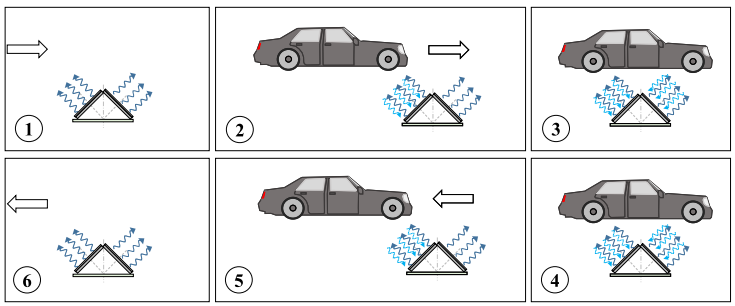

Fig. 9. Schematic of dual microwave Doppler radar vehicle detection.

DOI: 10.1587/elex.13.20161087
Received November 8, 2016
Accepted November 24, 2016
Publicized December 12, 2016
Copyedited January 10, 2017

As shown in Fig. 9, the microwave Doppler radar vehicle detection sensor was fixed in the center of a parking space. The vehicle motion recognition procedure was divided into six steps as following:

I. The parking space was vacant. Both radar "A" and "B" detected nothing.

II. A vehicle was moving into the parking space, but the sensor had not yet been covered by the moving vehicle. One of the radar module, either "A" or "B" depending on who was facing to the coming vehicle, detected the moving vehicle while the other one detected nothing.

III. The vehicle had moved into the parking space and covered the sensor. With the moving of the vehicle, both radar "A" and "B" detected it, and would lose it simultaneously once it stopped, which indicated the parking space was occupied.

IV. The parking space was occupied. Both radar "A" and "B" detected no vehicle movement. If the vehicle was ready to drive out from the parking space, it would be started on and move on the parking space firstly. Because the sensor was covered by the moving vehicle. Both radar "A" and "B" would detect the moving vehicle simultaneously, which indicated that the vehicle was driving out from the parking space.

V. The vehicle had moved out from the parking space. The sensor was exposed from the moving vehicle. But one of the radar module, "A" or "B" depending on whose detection axis was pointing to the leaving vehicle, detected the moving vehicle while the other one detected nothing.

VI. With the vehicle moving out of the parking space, the radar module whose detection axis was pointing to the leaving vehicle would lose target subsequently, which indicated that the parking space was vacant.

As shown in Fig. 7, the voltage outputs V_A and V_B from the signal amplifier of each radar module were input to the ADC of a MCU. Let T to be the ADC sample period and t the serial number of the sample data. DA(t) and DB(t) were the output data of radar "A" and "B" from ADC at tT moment, as shown in Fig. 10(a). To trace the radar signal and run the motion recognition algorithm, a W second detection time window was set to monitor the real-time output data from ADC,

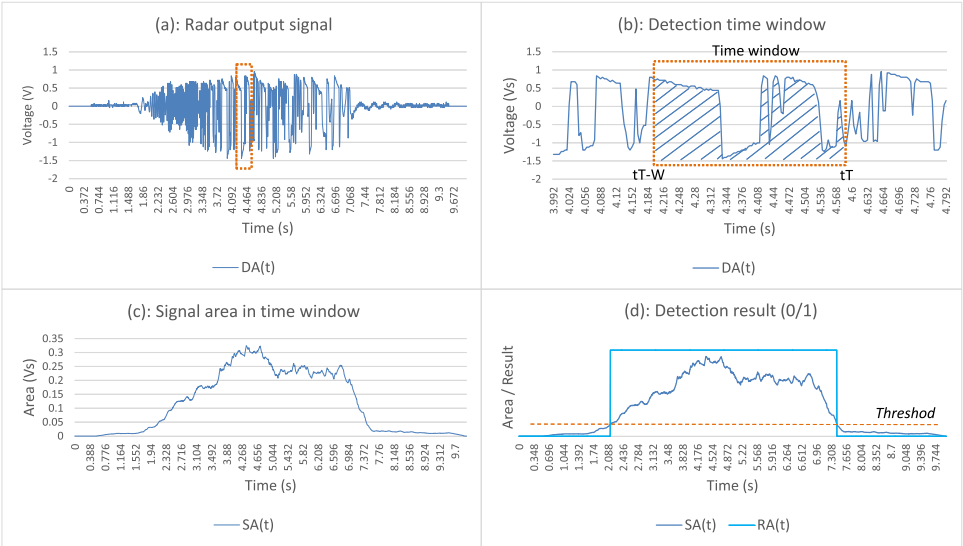

Fig. 10. Radar output signal processing.

DOI: 10.1587/elex.13.20161087
Received November 8, 2016
Accepted November 24, 2016
Publicized December 12, 2016
Copyedited January 10, 2017

as shown in Fig. 10(b). The area below the signal curve within the time window could be defined by equation (2), (3), as shown in Fig. 10(c).

$$SA(t) = \sum_{i=t-W/T-1}^{t} [|DA(i)| \times T] \tag{2}$$

$$SB(t) = \sum_{i=t-W/T-1}^{t} [|DB(i)| \times T] \tag{3}$$

If there was no vehicle movement detected by the radar modules, the background data was close to 0. Thus the area below the background signal was about 0. To avoid the influence of background signal fluctuation and improve the algorithm stability, a detection threshold $\xi = 0.05$ was introduced as an empirical value in our experiments. The radar "A" detection result RA(t), as shown in Fig. 10(d), and radar "B" detection result RB(t), was generated by comparing the area covered by the time window with the threshold ξ.

$$RA(t) = \begin{cases} 0, & SA(t) \le \xi \\ 1, & SA(t) > \xi \end{cases} \tag{4}$$

$$RB(t) = \begin{cases} 0, & SB(t) \le \xi \\ 1, & SB(t) > \xi \end{cases} \tag{5}$$

In our experiments, T was set to 0.004 s and W was set to 0.4 s. Two buffers, DA[100] and DB[100], were defined to save the sample data of V_A and V_B in the detection time window respectively. The value of RA(t), 1 or 0, indicated whether

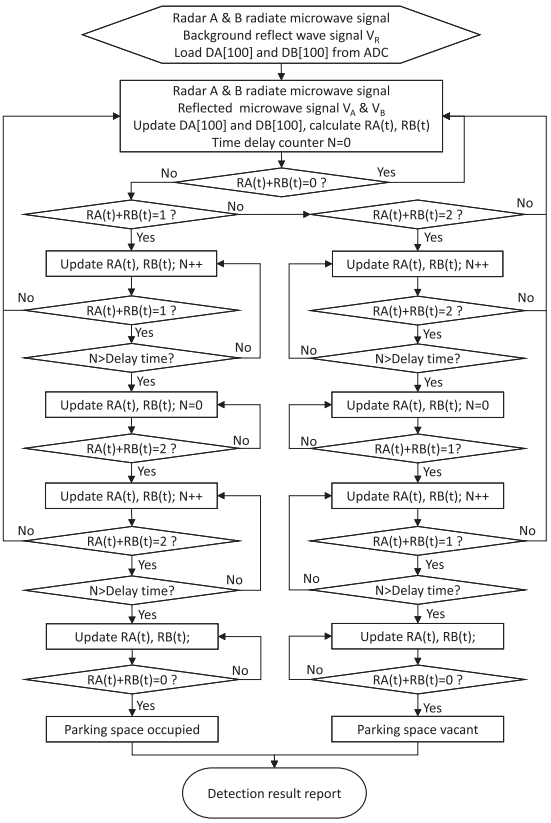

Fig. 11. Parking vehicle motion recognition algorithm.

DOI: 10.1587/elex.13.20161087
Received November 8, 2016
Accepted November 24, 2016
Publicized December 12, 2016
Copyedited January 10, 2017

a moving vehicle was detected by radar "A" or not, and so was RB(t). The parking vehicle motion recognition algorithm, shown in Fig. 11, was based on the value of RA(t) and RB(t), the sequence of the moment when the results occurred and the time the status lasted. In order to filter the instantaneous short time interference, the width of the time window, W, was used as a delay time in the algorithm.

4 Experimental results and analysis

Experiments based on the developed occupancy sensor, shown in Fig. 8, were implemented by mounting it in the center of a parking space with its radar module "A" detection direction pointing to the outside of the parking space and "B" to the inside, shown in Fig. 12. A Tektronix oscilloscope TDS2024C was connected to the signal processing circuit outputs of the two radar module "A" and "B" to display the output signal "V_A" and "V_B". And an Octavia car of Volkswagen SKODA was employed as a test vehicle.

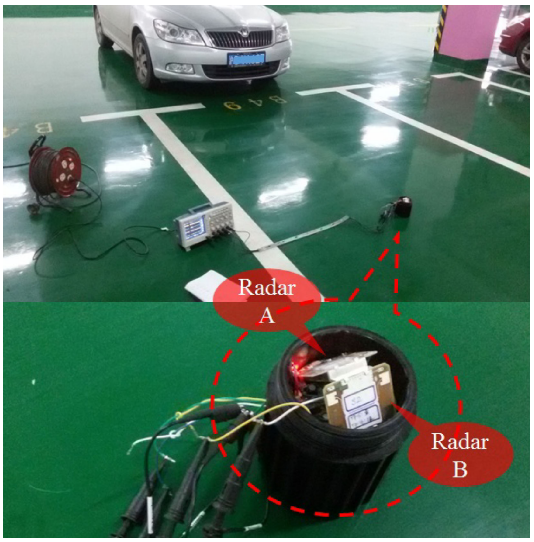

Fig. 12. Dual microwave Doppler radar sensor occupancy detection experiment.

Fig. 13 shows the signal output and its change processing of the two radar module "A" and "B" synchronously when the test car was driving to a vacant parking space and driving out from the space in our experiments.

As shown in Fig. 13(a), (c), (e), at first, since the parking space was vacant, the value of both radar "A" output DA(t) and radar "B" output DB(t) were background level. In phase 1, the car was coming to the parking space, radar "A" output signal DA(t) fluctuation amplitude reached to 1 V, while radar "B" output signal DB(t) kept in background level. The area below the DA(t) curve during the detection time window, SA(t), started to increase, while SB(t) kept near the background value. As the value of SA(t) increased to the detection threshold ξ, the movement detection result RA(t) = 1, while RB(t) kept 0. In phase 2, the car was driving into the parking space, covered the sensor and kept moving on the space, DA(t) kept it status while DB(t) fluctuation amplitude reached to about 1 V. As the value of SB(t) increased to the detection threshold ξ, RB(t) = 1, while RA(t) kept in 1. In phase 3,

DOI: 10.1587/elex.13.20161087
Received November 8, 2016
Accepted November 24, 2016
Publicized December 12, 2016
Copyedited January 10, 2017

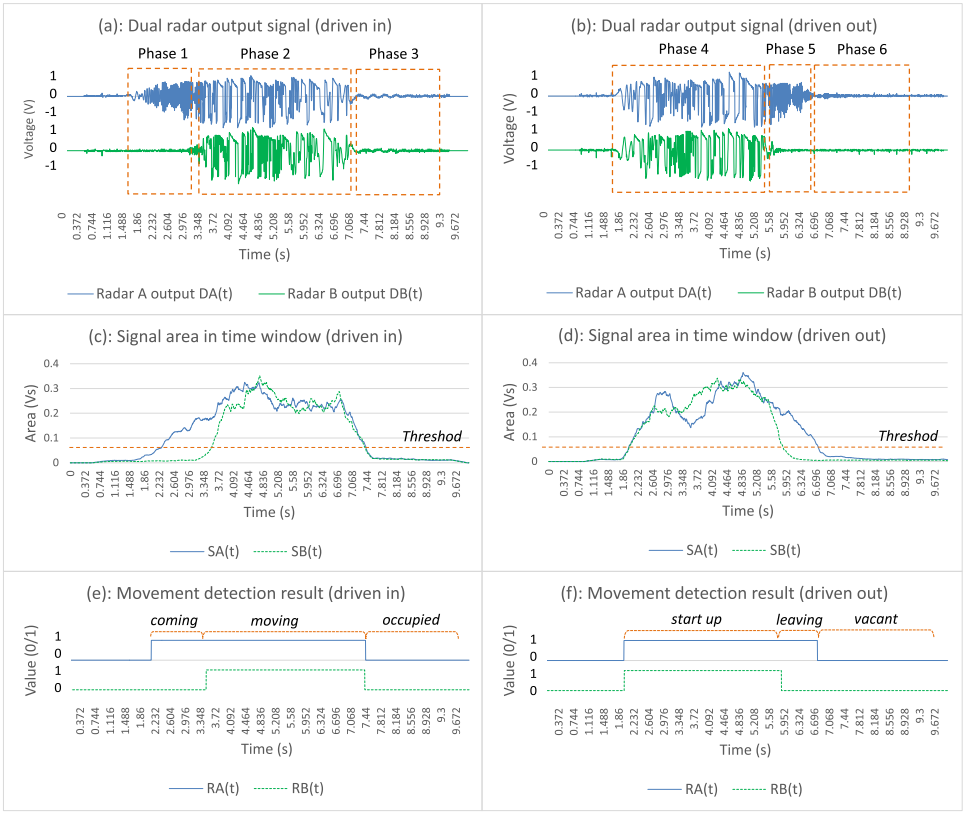

Fig. 13. Dual radar output signal and the processing result when a car was driven into or out of the parking space

the car stopped on the parking space, DA(t) and DB(t) went back to background value simultaneously. Both SA(t) and SB(t) started to fall back to background value at a similar rate. As SA(t) and SB(t) dropped blew the threshold ξ, RA(t) and RB(t) turned from 1 to 0. The parking space was occupied.

As shown in Fig. 13(b), (d), (f), after a period of time, in phase 4, the car was started up and moving in the parking space, both DA(t) and DB(t) fluctuation amplitude reached to about 1 V. SA(t) and SB(t) started to rise at a similar rate and reached to detection threshold ξ, at which point RA(t) and RB(t) changed from 0 to 1. In phase 5, the sensor was exposed from the coverage of the car chassis and the car was leaving from the parking space, radar "B" lost target and DB(t) fell back to background level. DA(t) kept its fluctuation amplitude about 1 V. SB(t) started to fall back to background value and reached to detection threshold ξ ahead of SA(t), which generated detection results of RB(t) = 0 and RA(t) = 1. In phase 6, as radar "A" lost target and DA(t) went back to background level, SA(t) dropped blew the threshold ξ, RA(t) = 0. The car was driven out and the parking space was vacant.

To test the detection accuracy of our design, we used six different types of vehicles to implement the experiments. The occupancy rate was tested when cars were driven into the parking space where the vehicle detection sensor mounted, and the vacant detection rate was measured afterward when cars were driven out. The detection accuracy rate is defined by equation (6). Table I shows the detection results for different type of vehicles.

DOI: 10.1587/elex.13.20161087
Received November 8, 2016
Accepted November 24, 2016
Publicized December 12, 2016
Copyedited January 10, 2017

$$Accuracy\_Rate = \frac{Occupied/Vacant\_Detection}{Parking\_Test\_Times}. \quad (6)$$

The detection results show that the proposed dual microwave Doppler radar based vehicle detection sensor has achieved more than 98% accuracy rate for both occupancy and vacant detection.

Table I. Parking space occupancy detection results of different vehicles

Vehicle type	Parking test times	Occupied detection	Accuracy rate	Vacant detection	Accuracy rate
Octavia SKODA	163	160	98.16%	161	98.77%
Cruze Chevrolet	156	153	98.08%	154	98.72%
MengDiOu Ford	103	102	99.03%	101	98.06%
GL8 Buick MPV	111	109	98.2%	110	99.1%
Tiguan Volkswagen SUV	49	49	100%	49	100%
Accord Honda	51	50	98.04%	50	98.04%

5 Conclusion

This paper proposed a dual microwave Doppler radar based vehicle detection sensor design and a motion recognition algorithm for parking lot occupancy detection. In contrast to the existing techniques, such as magnetometer and optical sensor, our work made contribution to the simplification of engineering integration from complex optical system design as well as achievement of high detection accuracy. In our design, dual microwave Doppler radar transceiver modules were employed to detect the movement of a parking vehicle. Based on the output signals of the two radar module, a motion recognition algorithm was designed to generate the parking space occupancy status. Our experiments suggested that the proposed dual microwave Doppler radar based vehicle detection sensor were able to detect the movement of a parking vehicle clearly while keeping the occupancy detection accuracy higher than 98%. For the future, we plan to employ the integrated magnetometer inside of the sensor to trigger the operation of the radar modules so that a battery powered parking lot occupancy sensor with higher detection accuracy but low energy consumption can be developed.

DOI: 10.1587/elex.13.20161087
Received November 8, 2016
Accepted November 24, 2016
Publicized December 12, 2016
Copyedited January 10, 2017